Structural Engineering and Mechanics, *Vol. 49, No. 5 (2014) 537-554*
DOI: http://dx.doi.org/10.12989/sem.2014.49.5.537

Higher order free vibration of sandwich curved beams with a functionally graded core

K. Malekzadeh Fard*

Department of Structural Analysis and Simulation, Space Research Institute, Malek Ashtar University of Technology, Tehran-Karaj Highway, PO Box. 14665-143, Tehran, Iran

(Received July 25, 2013, Revised October 25, 2013, Accepted December 9, 2013)

Abstract. In this paper, free vibration of a sandwich curved beam with a functionally graded (FG) core was investigated. Closed-form formulations of two-dimensional (2D) refined higher order beam theory (RHOBT) without neglecting the amount of *z/R* was derived and used. The present RHOBT analysis incorporated a trapezoidal shape factor that arose due to the fact that stresses through the beam thickness were integrated over a curved surface. The solutions presented herein were compared with the available numerical and analytical solutions in the related literature and excellent agreement was obtained. Effects of some dimensionless parameters on the structural response were investigated to show their effects on fundamental natural frequency of the curved beam. In all the cases, variations of the material constant number were calculated and presented. Effect of changing ratio of core to beam thickness on the fundamental natural frequency depended on the amount of the material constant number.

Keywords: free vibration; sandwich curved beam; FG- core; refined higher order beam

1. Introduction

Functionally graded materials (FGM) are microscopically inhomogeneous composites made from a mixture of materials by gradually varying volume fraction of the mixture and presenting smooth changes of properties from one side to another, which eliminates interface discontinuity problems. Natural frequencies are the basic and substantial issue for the design and use of such structural components, due to which free vibration of curved beams has been attracted intensive researches during the past few decades. Ahmed (1971) evaluated vibration characteristics of curved sandwich beams using finite elements with three to five degrees of freedom per node. He studied effects of factors such as core-to-face density ratio, core rigidity, core-to-face thickness and subtended angle on arch frequency. Many theories have been evolved to derive, simplify and solve the equations of motion for the free in-plane vibrations of the curved beams. In some of the studies, governing equations of motion are solved using the Rayleigh–Ritz method. Henrych (1981) derived the general expression of the equations of motion for a uniform circular arc based on the first-order equilibrium condition. Balasubramanian and Prathap (1989) explored the locking and field-consistency aspects of a shear flexible curved beam element for the vibration of stepped

*Corresponding author, Associate Professor, E-mail: k.malekzadeh@gmail.com

http://www.techno-press.org/?journal=sem&subpage=8 ISSN: 1225-4568 (Print), 1598-6217 (Online)

arches. Qatu (1993) developed an exact as well as Ritz method-based approximate solutions for the vibration of laminated composite arches. He reported that, since the effects of shear deformation and rotatory inertia are neglected, natural frequencies may be inaccurate for a moderately deep arch with relatively soft transverse shear modulus and for highly anisotropic composites. In order to take into account these effects, the first order shear deformation theory for moderately deep arches was developed by Qatu. But it was failed to consider the trapezoidal shape factor $(1+z/R)$ that arise due to the fact that the stresses over the thickness of the curved beam have to be integrated on cross-section of a curved beam element to obtain the accurate stress-resultants.

Auciello and Rosa (1994) ignored the shear deformation and rotary inertia, and assumed that the curved axis is incompressible. They studied the vibrations of classical arches through Galerkin, Ritz and finite element methods. They examined the influence of cross-sectional variations and of flexible supports on the vibration of arches. Krishnan and Dharmaraj (1995) explored the role of subtended angle on the fundamental frequency of arches, with various end conditions. Khdeir and Reddy (1997) developed a third order theory for vibration studies of shallow composite arches (HOAT) which could be reduced to classical arch theory (CAT) and second order arch theory (SOAT) with proper definition of deformation parameters. Higher order shear deformation theories (HOAT) are good in predicting natural frequencies of slightly shallow thick laminated curved beams; but, they are unable to predict natural frequencies of thick laminated curved beams.

Krishnan and Suresh (1998) developed a cubic element to study the effects of curvature, shear deformation and rotary inertia on the fundamental frequency of curved beams. Based on the Timoshenko-type curved beam theory, Tseng *et al*. (2000) applied the stiffness analysis method involving shear deformation and rotation inertia to determine the natural frequencies of laminated beams with arbitrary curvatures.

Eisenberger and Efraim (2001) studied the uniform circular beams using the Timoshenko beam theory, which includes the effects of rotary inertia, shear deformation, and the couplings of the radial and tangential displacements. It has been shown that the Timoshenko beam theory provides a better approximation to the actual behavior of beams, in which the effect of the cross-sectional dimension on frequencies cannot be neglected, and the study of high modes is required.

Kang and Riedel (2003) established however that the application of classical arch theory (CAT) is highly confined to slender geometry due to the Kirchhoff hypothesis where the shear deformation and rotary inertia are neglected. As a result, the deflection is always under-estimated while the natural frequencies and buckling loads are over-predicted. Lu *et al*. (2008) presented an exact analysis for the in-plane free vibration of simply supported laminated circular arches based on the two-dimensional theory of elasticity using the state space method. The method of separation of variables is employed to expand all the variables into Fourier series about the longitudinal coordinate, so that the system of partial differential equations is reduced to the ordinary one about the radial coordinate. This solution does not adopt any assumptions about the distribution of displacements of strains along the thickness direction. Sudhakar *et al*. (2008) studied the free vibrations of sandwich and composite arches base on higher-order model with finite element modeling with transverse shear and normal strain components. In this formulation $(1+z/R)$ term (trapezoidal shape factor) in the shear strain is neglected. Although the first-order arch theories (FOATs) by regarding the shear deformation as constant through the thickness direction, the accuracy of results are highly dependent on the choice of shear correction factor and the determination of the latter is a rather cumbersome task. In addition, the FOATs are only applicable to thin and moderately thick laminates but not to strongly thick arches. FG materials absolutely have potential applications in various industries such as aerospace engineering, automobile

industry and mechanical metallurgy, however, their manufacturability and applicability is still in among scientists (Koizumi 1993).The most important advantage of a monotonous variation of volume fraction of constituent phases is elimination of stress discontinuity that is often encountered in laminated composites and, accordingly, avoiding delamination-related problems. FGM may be also developed using fiber-reinforced layers with volume fraction of fibers that is coordinate-dependent, rather than constant, producing an optimal set of properties or responses (Birman 1995). Many attempts have been done in case of an FGM beam. Sankar (2001) investigated an FGM beam subjected to a sinusoidal transverse load applied at one of the surfaces. Exact elasticity solution for stresses and displacements was compared with the results obtained by technical Bernoulli–Euler beam theory. The impact of a sandwich beam with isotropic homogeneous facings and a functionally graded core was considered by Apetre *et al*. (2006). Modulus of elasticity of the core was represented by a polynomial function of thickness coordinate while its Poisson ratio was assumed constant. Aydogdu and Taskin (2007) presented free vibrations of FGM beams with simply supported edges. Li (2008) investigated static and dynamic behaviors of an FGM Bernoulli–Euler and Timoshenko beam. Malekzadeh *et al*. (2009) solved free vibration of a thick FGM circular beam subjected to thermal heat by means of 2D elasticity theory and used differential quadrature method (DQM). Malekzadeh *et al*. (2010) applied a formulation based on first order shear deformation including effect of rotary inertia for out of plane free vibration of functionally graded circular curved beam in the thermal environment. Kiani *et al*. (2012) analyzed functionally graded material doubly curved panel based on first order shear deformation theory for thermoelastic free vibration and dynamic analysis.

The purpose of this work is to develop a refined higher order theory for deep and thick laminated composite and sandwich curved beam with FG core, which could account for effects of transverse shear strains/stresses and transverse normal strain/stress. The theory included a two-dimensional (2D) displacement field with up to eight degrees of freedom. Since the cross-sectional warping was accurately modeled in this theory, it did not require any shear correction factor. The equations included accurate stress-resultant equations for composite thick circular curved beams where $(1+z/R)$ terms were included in the stress-resultant equations and exactly integrated. Equations of motion and boundary conditions were derived using Hamilton's principle. In this paper, after deriving RHOBT for free vibrations of a sandwich curved beams with FG soft core, the problem was solved by Fourier series and Navier's method and the results were obtained by means of a generated code. In order to validate the proposed approach and explore the limits of applicability, natural frequencies were obtained for wide ranges of length-to-radius and thickness-to-radius ratios and were compared with the values published in the open literature. Furthermore, the present method did not require any convergence study, which was in contrast to some other higher order theories for free vibration analyses reported in the literature.

2. Modeling FG material properties

Material properties of FGMs are continuously varying through thickness. So, Young's modulus and Poisson's ratio are functions of z as the coordinate system varies from $-h/2$ to $h/2$ (one side to another). Some mathematical models have been presented by investigators in order to show variations of material properties of FGM plates. P-FGM (Bao and Chung 1995) and S-FGM (Chi and Chung 2003) are such models. In the present work, Mori-Tanaka's (1973) scheme, which is a more realistic determination technique (Golmakani and Kadkhodayan 2011), was taken into

account. The Mori-Tanaka scheme for estimating the effective moduli is applicable to regions of the graded microstructures which have a well-defined continuous matrix and a discontinuous particulate phase. It takes in to account the interaction of the elastic fields among neighboring inclusions (Shen 2009). This homogenization method is presented as follows

$$\begin{aligned}
&\frac{K-K_1}{K_2-K_1}=\frac{V_2}{1+\dfrac{3(1-V_2)(K_2-K_1)}{3K_1+4G_1}}\\
&\frac{G-G_1}{G_2-G_1}=\frac{V_2}{1+3(1-V_2)(G_2-G_1)/(G_1-f_1)}\\
&f_1=G_1(9K_1+8G_1)/6(K_1+2G_1)
\end{aligned} \tag{1}$$

in which K is effective bulk modulus, G is effective shear modulus and V is volume fraction of the FGM beam. Index 1 shows properties of the top and index 2 is for the bottom of the beam. The volume fractions, according to the power law, are assumed as

$$\begin{cases} V_1=\left(\dfrac{1}{2}-\dfrac{z}{h}\right)^k \\ V_2=1-V_1 \end{cases} \tag{2}$$

k is a material constant. Based on the presented method, effective values of Young's modulus, E, and Poisson's ratio, ν, are computed using

$$\begin{aligned}
&E=9KG/(3K+G)\\
&\nu=(3K-2G)/2(3K+G)
\end{aligned} \tag{3}$$

So that top face of the FGM core is fully from material 1 and its bottom face is fully from material 2; k describes various volume fractions between these two faces.

3. Geometrical description

Fig. 1 shows a sandwich curved beam with an FGM core. (x, z, φ) denote polar co-ordinates, where φ curve lies in mid-surface of the beam, x curve lies across width of the beam and z is perpendicular to these two curves in the thickness direction. Consider a k-layered laminated circular curved beam with a total thickness of h, and each layer having the thickness of h_k, as depicted in Fig. 1. R represents principal radius of the mid-surface curvature along φ direction. The beam is considered to be a 2D elastic medium.

3.1 Displacement field

The higher-order displacement model, based on Taylor's series expansion is used to deduce a 2D formulation of a 3D elasticity problem and the following set of equations are obtained by expanding the displacement components $u(\phi, z, t)$ and $w(\phi, z, t)$ of any point in the curved beam space in terms of the thickness coordinate z

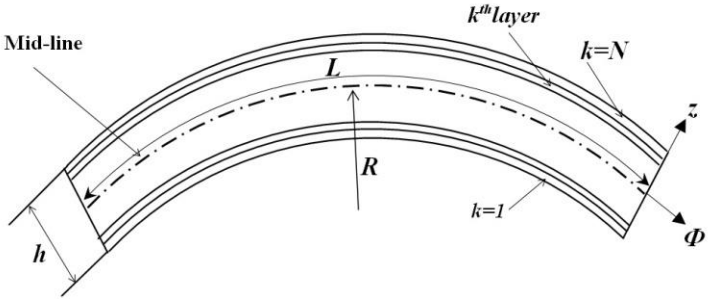

Fig. 1 Sandwich curved beam with a FG core

$$\begin{aligned} u(\varphi,z,t) &= (1+z/R)u_0(\varphi,t) + z\theta_\varphi(\varphi,t) + z^2u_0^*(\varphi,t) + z^3\theta_\varphi^*(\varphi,t) \\ w(\varphi,z,t) &= w_0(\varphi,t) + z\theta_z(\varphi,t) + z^2w_0^*(\varphi,t) + z^3\theta_z^*(\varphi,t) \end{aligned} \tag{4}$$

in which u and w are displacements of a general point in the laminate and t is time. u_0 is axial displacement relating to the mid-line and w_0 is transverse displacement of a point on the mid-line. Other terms such as θ_φ, θ_z, u^*_0, w^*_0, θ^*_φ and θ^*_z are the functions which are defined in the mid-surface and are represented as follows

$$\begin{aligned} \theta_\varphi &= \frac{\partial u}{\partial z}\Big|_{z=0} \qquad u_0^* = \frac{1}{2}\frac{\partial^2 u}{\partial z^2}\Big|_{z=0} \qquad \theta_\varphi^* = \frac{1}{6}\frac{\partial^3 u}{\partial z^3}\Big|_{z=0} \\ \theta_z &= \frac{\partial w}{\partial z}\Big|_{z=0} \qquad w_0^* = \frac{1}{2}\frac{\partial^2 w}{\partial z^2}\Big|_{z=0} \qquad \theta_z^* = \frac{1}{6}\frac{\partial^3 w}{\partial z^3}\Big|_{z=0} \end{aligned} \tag{5}$$

As shown in the equation of displacement field (Eq. (4)), the amount of z compared to the radii of curvatures ($z/R \neq 0$) is not negligible. With the use of definition of strains from the linear theory of elasticity for circular curved beams that is deduced from a linear theory of elasticity for cylindrical shell, the general strain–displacement relations in the cylindrical coordinate system are given as follows

$$\begin{aligned} \varepsilon_\varphi &= \frac{1}{1+z/R}\left(\frac{1}{R}\frac{\partial u}{\partial \varphi} + \frac{1}{R}w\right) \\ \gamma_{\varphi z} &= \frac{1}{1+z/R}\left(\frac{1}{R}\frac{\partial w}{\partial \varphi} - \frac{u}{R}\right) + \frac{\partial u}{\partial z} \\ \varepsilon_z &= \frac{\partial w}{\partial z} \end{aligned} \tag{6}$$

Substituting displacement field equations in these equations yields linear strains in terms of mid-line displacement

$$\begin{aligned} \varepsilon_\varphi &= \frac{1}{1+\gamma_0 z/R}(\varepsilon_{\varphi 0} + z\chi_\varphi + z^2\varepsilon_{\varphi 0}^* + z^3\chi_\varphi^*) \\ \gamma_{\varphi z} &= \frac{1}{1+\gamma_0 z/R}(\beta_{\varphi 0} + z\chi_{\varphi z0} + z^2\beta_{\varphi 0}^* + z^3\chi_{\varphi z0}^*) + (\beta_{\varphi 1} + z\chi_{\varphi z1} + z^2\beta_{\varphi 1}^*) \\ \varepsilon_z &= (\varepsilon_{z0} + z\chi_z + z^2\varepsilon_{z0}^*) \end{aligned} \tag{7}$$

in which

$$\varepsilon_{\varphi 0}=(\frac{1}{R}\frac{\partial u_0}{\partial \varphi}+\frac{1}{R}w_0),\quad \chi_{\varphi}=\gamma_0\frac{1}{R^2}\frac{\partial u_0}{\partial \varphi}+\frac{1}{R}\frac{\partial \theta_{\varphi}}{\partial \varphi}+C_1\frac{1}{R}\theta_z,\quad \varepsilon^*_{\varphi 0}=(\frac{1}{R}\frac{\partial u_0^*}{\partial \varphi}+C_1\frac{1}{R}w_0^*)$$
$$\chi^*_{\varphi}=\frac{1}{R}\frac{\partial \theta^*_{\varphi}}{\partial \varphi}+C_2\frac{1}{R}\theta^*_z,\quad \beta_{\varphi 0}=\frac{1}{R}\frac{\partial w_0}{\partial \varphi}-\frac{1}{R}u_0,\quad \chi_{\varphi z0}=C_1\frac{1}{R}\frac{\partial \theta_z}{\partial \varphi}-\gamma_0\frac{1}{R^2}u_0-\frac{1}{R}\theta_{\varphi}$$
$$\chi^*_{\varphi z0}=C_2\frac{1}{R}\frac{\partial \theta^*_z}{\partial \varphi}-\frac{1}{R}\theta^*_{\varphi},\quad \beta^*_{\varphi 0}=C_1\frac{1}{R}\frac{\partial w_0^*}{\partial \varphi}-\frac{1}{R}u_0^*,\quad \varepsilon_{z0}=C_1\theta_z,\quad \varepsilon^*_{z0}=3C_2\theta^*_z \tag{8}$$
$$\beta_{\varphi 1}=(\gamma_0\frac{1}{R}u_0+\theta_{\varphi}),\quad \chi_{\varphi z1}=2u_0^*,\quad \chi_z=2C_1w_0^*,\quad \beta^*_{\varphi 1}=3\theta^*_{\varphi}$$

For stress-strain relations, by assuming principal material axes (1,2,3) and laminate general axes (x, y, z) in the curvilinear co-ordinate system, stress-strain relations for the K^{th} lamina in the principal material co-ordinates for the theory was developed by Garg *et al*. (2006)

$$\left\{\sigma_{ij}\right\}^K=\left[C_{ij}\right]^K\left\{\varepsilon_{ij}\right\}^K \tag{9}$$

where C_{ij} components are also available in (Garg *et al*. 2006). After transforming constitutive relations from the lamina principal axes (1, 2, 3) to the laminate general axes, the following can be obtained

$$\sigma=Q\varepsilon \tag{10}$$

where coefficients of Q matrix are reduced elastic constants of orthotropic material of the K^{th} lamina, as defined by Garg *et al*. (2006). Integrating Eq. (6) over thickness of the shell gives

$$\overline{\sigma}=D\overline{\varepsilon} \tag{11}$$

in which (Garg *et al*. 2006)

$$\overline{\sigma}=(N_{\varphi},N^*_{\varphi},C_1N_z,C_2N^*_z,M_{\varphi},M^*_{\varphi},M_z,Q_{\varphi},R_{\varphi},Q^*_{\varphi},R^*_{\varphi},S_{\varphi},T_{\varphi},S^*_{\varphi})^t$$
$$\overline{\varepsilon}=(\varepsilon_{\varphi 0},\varepsilon^*_{\varphi 0},C_1\varepsilon_{z0},C_2\varepsilon^*_{z0},\chi_{\varphi},\chi^*_{\varphi},\chi_z,\beta_{\varphi 0},\beta_{\varphi 1},\beta^*_{\varphi 0},\beta^*_{\varphi 1},\chi_{\varphi z0},\chi_{\varphi z1},\chi^*_{\varphi z0})^t \tag{12}$$

and D matrix is defined as follows by Garg *et al.* (2006)

$$D=\begin{bmatrix}D_f & 0\\ 0 & D_s\end{bmatrix} \tag{13}$$

$\overline{\boldsymbol{\varepsilon}}$ and $\overline{\boldsymbol{\sigma}}$ are the vectors of mid-surface strains and stress resultants, respectively, and the matrices $\mathbf{D_f}$ and $\mathbf{D_s}$ for various displacement models are given in Appendix A. Accurate method of calculation of the integrals in stress-resultant equations including the (1+z/R) terms (in the denominator of the stress-resultant integrands) are explained in Appendix B. Also, Components of Eq. (13) are available in the paper by Khalili *et al*. (2011). Here, calculation process of D depends on Eq. (1) and is stiffness matrix of the curved sandwich beam with a FG core. Therefore, the stress resultant components for the laminate consist of N layers in the form of doubly-curved shell as defined below

$$
\begin{aligned}
&(R_\varphi \quad T_\varphi \quad R_\varphi^*) = \sum_{k=1}^{NL}\int_{z_k}^{z_{k+1}} \sigma_{\varphi z}(1, z, z^2)(1+\gamma_0 z/R)dz \\
&\begin{bmatrix} N_\varphi & M_\varphi & N_\varphi^* & M_\varphi^* \\ Q_\varphi & S_\varphi & Q_\varphi^* & S_\varphi^* \end{bmatrix} = \sum_{k=1}^{NL}\int_{z_k}^{z_{k+1}} \begin{Bmatrix} \sigma_\varphi \\ \sigma_{\varphi z} \end{Bmatrix}(1, z, z^2, z^3)dz \\
&(N_z, M_z, N_z^*) = \sum_{k=1}^{NL}\int_{z_k}^{z_{k+1}} \sigma_z(1, z, z^2)(1+\gamma_0 z/R)dz
\end{aligned}
\tag{14}
$$

3.2 Shell kinematics

Hamilton's principal is used to define equations of motion with respect to the displacement field in Eq. (1). The analytical form is stated as follows by Sudhakar *et al*. (2008)

$$
\int_0^t \delta L dt \equiv \int_0^t \left[(\delta K) - (\delta U)\right] dt = 0 \tag{15}
$$

where δK denotes the first variation of virtual kinetic energy and δU the first variation of virtual strain energy. Substituting the appropriate energy expressions, the final expressions can be written as

$$
\begin{aligned}
&\delta\left(\frac{1}{2}\int_0^t \int_{-h/2}^{h/2}\int_A \rho[\dot{u}^2 + \dot{w}^2]dA.dz.dt - \frac{1}{2}\int_0^t \int_{-h/2}^{h/2}\int_A [\sigma_\phi \varepsilon_\phi + \sigma_z \varepsilon_z + \sigma_{\phi z}\varepsilon_{\phi z}]dA.dz.dt\right) = 0 \\
&dA = b.R.(1+z/R)\,d\phi
\end{aligned}
\tag{16}
$$

Where ρ is the mass density of the material of the laminate and the superposed dots denote differentiation with respect to time. Substituting the appropriate strain expressions given by Eqs. (6)-(9) and the displacement expressions given by Eq. (1) in Eq. (16), integrating the resulting expression by parts and collecting the coefficients of δu_0, δw_0, $\delta\theta_x$, $\delta\theta_z$, δu^*_0, δw^*_0, $\delta\theta^*_x$, and $\delta\theta^*_z$ the following eight equations of motion are obtained

$$
\begin{aligned}
&\frac{1}{R}\frac{\partial N_\varphi}{\partial \varphi} + \frac{1}{R^2}\frac{\partial M_\varphi}{\partial \varphi} + \frac{1}{R}Q_\varphi - \frac{1}{R}R_\varphi + \frac{1}{R^2}S_\varphi + \frac{1}{R^2}N_\varphi^i \frac{\partial^2 u_0}{\partial \varphi^2} + \frac{2}{R^2}N_\varphi^i \frac{\partial w_0}{\partial \varphi} \\
&= \frac{\partial^2 u_0}{\partial t^2}(\bar{I}_0 + \frac{2}{R}\bar{I}_1 + \frac{1}{R^2}\bar{I}_2) + \frac{\partial^2 \theta_\varphi}{\partial t^2}(\bar{I}_1 + \frac{1}{R}\bar{I}_2) + \frac{\partial^2 u_0^*}{\partial t^2}(\bar{I}_2 + \frac{1}{R}\bar{I}_3) + \frac{\partial^2 \theta_\varphi^*}{\partial t^2}(\bar{I}_3 + \frac{1}{R}\bar{I}_4)
\end{aligned}
$$

$$
-\frac{1}{R}N_\varphi + \frac{1}{R}\frac{\partial Q_\varphi}{\partial \varphi} - \frac{2}{R^2}N_\varphi^i \frac{\partial u_0}{\partial \varphi} + \frac{1}{R^2}N_\varphi^i \frac{\partial^2 w_0}{\partial \varphi^2} = \frac{\partial^2 w_0}{\partial t^2}\bar{I}_0 + \frac{\partial^2 \theta_z}{\partial t^2}\bar{I}_1 + \frac{\partial^2 w_0^*}{\partial t^2}\bar{I}_2 + \frac{\partial^2 \theta_z^*}{\partial t^2}\bar{I}_3
$$

$$
\frac{1}{R}\frac{\partial M_\varphi}{\partial \varphi} + \frac{1}{R}S_\varphi - R_\varphi = \frac{\partial^2 u_0}{\partial t^2}(\bar{I}_1 + \frac{1}{R}\bar{I}_2) + \frac{\partial^2 \theta_\varphi}{\partial t^2}\bar{I}_2 + \frac{\partial^2 u_0^*}{\partial t^2}\bar{I}_3 + \frac{\partial^2 \theta_\varphi^*}{\partial t^2}\bar{I}_4
$$

$$
-\frac{1}{R}M_\varphi - N_z + \frac{1}{R}\frac{\partial S_\varphi}{\partial \varphi} = \frac{\partial^2 w_0}{\partial t^2}\bar{I}_1 + \frac{\partial^2 \theta_z}{\partial t^2}\bar{I}_2 + \frac{\partial^2 w_0^*}{\partial t^2}\bar{I}_3 + \frac{\partial^2 \theta_z^*}{\partial t^2}\bar{I}_4
$$

$$\frac{1}{R}\frac{\partial N_{\varphi}^{*}}{\partial \varphi}+\frac{1}{R}Q_{\varphi}^{*}-2T_{\varphi}=\frac{\partial^2 u_0}{\partial t^2}(\bar{I}_2+\frac{1}{R}\bar{I}_3)+\frac{\partial^2 \theta_{\varphi}}{\partial t^2}\bar{I}_3+\frac{\partial^2 u_0^{*}}{\partial t^2}\bar{I}_4+\frac{\partial^2 \theta_{\varphi}^{*}}{\partial t^2}\bar{I}_5$$

$$-\frac{1}{R}N_{\varphi}^{*}-2M_z+\frac{1}{R}\frac{\partial Q_{\varphi}^{*}}{\partial \varphi}=\frac{\partial^2 w_0}{\partial t^2}\bar{I}_2+\frac{\partial^2 \theta_z}{\partial t^2}\bar{I}_3+\frac{\partial^2 w_0^{*}}{\partial t^2}\bar{I}_4+\frac{\partial^2 \theta_z^{*}}{\partial t^2}\bar{I}_5$$

$$\frac{1}{R}\frac{\partial M_{\varphi}^{*}}{\partial \varphi}+\frac{1}{R}S_{\varphi}^{*}-3R_{\varphi}^{*}=\frac{\partial^2 u_0}{\partial t^2}(\bar{I}_3+\frac{1}{R}\bar{I}_4)+\frac{\partial^2 \theta_{\varphi}}{\partial t^2}\bar{I}_4+\frac{\partial^2 u_0^{*}}{\partial t^2}\bar{I}_5+\frac{\partial^2 \theta_{\varphi}^{*}}{\partial t^2}\bar{I}_6$$

$$-\frac{1}{R}M_{\varphi}^{*}-3N_z^{*}+\frac{1}{R}\frac{\partial S_{\varphi}^{*}}{\partial \varphi}=\frac{\partial^2 w_0}{\partial t^2}\bar{I}_3+\frac{\partial^2 \theta_z}{\partial t^2}\bar{I}_4+\frac{\partial^2 w_0^{*}}{\partial t^2}\bar{I}_5+\frac{\partial^2 \theta_z^{*}}{\partial t^2}\bar{I}_6 \tag{17}$$

in which

$$\left(\bar{I}_0,\bar{I}_1,\bar{I}_2,\bar{I}_3,\bar{I}_4,\bar{I}_5,\bar{I}_6\right)=\sum_{k=1}^{NL}\int_{z_k}^{z_{k+1}}\rho_k\left(1,z,z^2,z^3,z^4,z^5,z^6\right)(1+z/R)dz \tag{18}$$

in which "*k*" shows layer number.

The local boundary conditions at the edges of the laminate are obtained simultaneously with the governing equations, as follows

$$\begin{aligned}
&\delta u_0=0 \quad \text{or} \quad \left(N_{\phi}+\gamma_0/RM_{\phi}\right)=0\\
&\delta w_0=0 \quad \text{or} \quad Q_{\phi}=0\\
&\delta \theta_{\varphi}=0 \quad \text{or} \quad M_{\phi}=0\\
&\delta \theta_z=0 \quad \text{or} \quad S_{\phi}=0\\
&\delta u_0^{*}=0 \quad \text{or} \quad N_{\phi}^{*}=0\\
&\delta w_0^{*}=0 \quad \text{or} \quad Q_{\phi}^{*}=0\\
&\delta \theta_{\varphi}^{*}=0 \quad \text{or} \quad M_{\phi}^{*}=0\\
&\delta \theta_z^{*}=0 \quad \text{or} \quad S_{\phi}^{*}=0
\end{aligned} \tag{19}$$

4. Solution of equations

In order to solve the derived equations, Navier solution by means of Fourier series was considered. For the simply supported beam, boundary conditions are explained as follows

$$w_0=w_0^{*}=\theta_z=\theta_z^{*}=\left(N_{\varphi}+1/RM_{\varphi}\right)=N_{\varphi}^{*}=M_{\varphi}=M_{\varphi}^{*}=0 \tag{20}$$

In order to satisfy the above conditions, Fourier series are set as

$$u_0(\varphi,t)=\sum_{n=1}^{\infty}u_{0n}\cos(\lambda\varphi)e^{i\omega_n t} \qquad u_0^*(\varphi,t)=\sum_{n=1}^{\infty}u_{0n}^*\cos(\lambda\varphi)e^{i\omega_n t}$$

$$w_0(\varphi,t)=\sum_{n=1}^{\infty}w_{0n}\sin(\lambda\varphi)e^{i\omega_n t} \qquad w_0^*(\varphi,t)=\sum_{n=1}^{\infty}w_{0n}^*\sin(\lambda\varphi)e^{i\omega_n t}$$

$$\theta_\varphi(\varphi,t)=\sum_{n=1}^{\infty}\theta_{\varphi n}\cos(\lambda\varphi)e^{i\omega_n t} \qquad \theta_\varphi^*(\varphi,t)=\sum_{n=1}^{\infty}\theta_{\varphi n}^*\cos(\lambda\varphi)e^{i\omega_n t}$$

$$\theta_z(\varphi,t)=\sum_{n=1}^{\infty}\theta_{zn}\sin(\lambda\varphi)e^{i\omega_n t} \qquad \theta_z^*(\varphi,t)=\sum_{n=1}^{\infty}\theta_{zn}^*\sin(\lambda\varphi)e^{i\omega_n t} \tag{21}$$

in which $\lambda=n\pi/a_0$ and polar angle which is φ varies from 0 to a_0. ω_n is natural frequency of the beam. Here, u_{0n}, w_{0n}, $\theta_{\phi n}$, θ_{zn}, u^*_{0n}, w^*_{0n}, $\theta^*_{\phi n}$, θ^*_{zn} are the amplitudes of the vibration; i is an imaginary unit; ω_n is a natural circular frequency of vibration measured in [rad/s]; n is an order of the natural vibration mode that defines its shape. Substituting Eq. (21) into equations of motion for different displacement models considered herein, and collecting coefficients, the eigenvalue equation is obtained as follows

$$\left[[\mathbf{K}]-\lambda_n[\mathbf{M}]\right]\{\mathbf{d}\}=\{\mathbf{0}\} \tag{22}$$

Where $\lambda_n=(\omega_n)^2$ and $\{\mathbf{d}\}$ is the displacement vector, for any value of n. The above eigenvalue equation can be solved for the various eigenvalues and associated eigenvectors. The lowest eigenvalue gives the square of the fundamental frequency of vibration. Some elements of the stiffness matrix [**K**] and the mass matrix [**M**] for the different displacement models are given in Appendix C.

5. Numerical results and discussion

This section consists of two parts. In the first part, verification is done and results of the present work are compared with those of other well-known investigators. The second part contains new results, derived by solving Eq. (22) of the present work, using a generated code. The number of Furrier series sentences was considered n=13 in all examples. For the first stage, a curved sandwich beam with length of 28 inches and curvature radius of 168.06 inches was selected with following material properties:

Face sheets: $E=1.0\times10^7\ lb/in^2$, $\rho=2.5098\times10^{-4}\ lbs^2/in^4$, $\nu=0.3$, $h_f(top,bot.)=0.018\ in$

Core: $G=12.0\times10^3\ lb/in^2$, $\rho=3.0717\times10^{-6}\ lbs^2/in^4$, $\nu=0.3$, $h_c=0.5\ in$

Results of the first five natural frequencies are listed in Table 1.

Table1 First five natural frequencies of a sandwich beam

Mode	Present work	Sudhakar *et al.* (2006)	Sakiyama (1997)	Ahmed (1971)
1	182.254	182.288	182.7	199.5
2	348.615	348.224	351.4	394.0
3	713.240	714.327	726.1	746.0
4	1137.187	1135.075	1162.0	1175.0
5	1588.470	1585.476	1633.0	1639.0

Table 2 Natural frequencies of a sandwich curved beam with FG core

k	**Mode**	*L/h*=10	*L/h*=100
1	1	4.0830	4.5893
	2	13.7775	18.5926
	3	25.1901	41.7420
	4	36.9678	73.7650
10	1	3.2441	3.5228
	2	11.6668	14.2736
	3	22.4810	32.1056
	4	34.1538	56.8948

As can be seen, results of the present work were so close to those of Sudhakar *et al*. (2006), especially in the case of fundamental natural frequency, which the discrepancy was less than 0.02%. Maximum discrepancy between results of the present work and Sakiyama (1997) was also less than 0.2%. The reason why the results of Sakiyama (1997) were higher than other results could be due to neglecting shearing deformation effect in the results. Ahmed (1971) used first order shear deformation theory and constant shear strains. Discrepancy for the fundamental natural frequency between Ahmed's (1971) study and the present work was about 0.2% and was maximum for the fifth mode which was less the 3%.

For the next part, a sandwich curved beam with an FGM core was selected. The layer arrangement was [0/90/Core- FGM /90/0] and *L/h*=10, 100, h_c/h=0.8, *L/R*=0.5. Material properties were as follows:

Top face sheet: $E_1 = 172.7\,Gpa, E_2 = 7.2\,Gpa, G_{12} = G_{13} = G_{23} = 3.76\,Gpa, \nu = 0.3, \rho = 1566\,kg/m^3$

Bottom face sheet:

$E_1 = 24.51\,Gpa, E_2 = 7.77\,Gpa, G_{12} = G_{13} = G_{23} = 3.34\,Gpa, \nu = 0.3, \rho = 1800\,kg/m^3$

FGM core:

$E_1 = 172.7\,Gpa, E_2 = 24.51\,Gpa, G_1 = 3.76\,Gpa, G_2 = 3.34\,Gpa, \nu = 0.3, \rho_1 = 1566\,kg/m^3, \rho_2 = 1800\,kg/m^3$

Non-dimensional factor of the natural frequency was also used as follows: $\Omega = \omega L^2 / h \times \left(\rho_c / E_c\right)^{0.5}$

Results of the first four natural frequencies for various *L/h* and various *k* are listed in Table 2.

In the next stage, based on the material and system properties used in Table 2, some parameters which influenced fundamental natural frequency of a curved sandwich beam with FGM core were investigated.

5.1 Effect of thickness ratio of core on fundamental natural frequency (h_c/h)

In lower amounts of *k*, by thickening core thickness compared to thickness of the beam, inertia moments of the section of the beam became greater; thus, flexural rigidity of the beam increased, which made raised fundamental natural frequency of the system. On the other hand, in higher amounts of *k*, increasing core thickness resulted in slightly lower fundamental natural frequencies. These variations are plotted for *L/R*=0.5 and *L/h*=10 in Fig. 2.

5.2 Effect of the length of the beam on the fundamental natural frequency (L/h)

Variations of the length of the beam for h_c/h=0.8 and L/R=0.5 are plotted on Fig. 3. As can be seen, for these range of material and system properties, increasing the length, makes the fundamental natural frequencies to be greater. By increasing the k, fundamental natural frequency of the system is decreased and also the ratio of increasing of the fundamental natural frequency due to increasing the length of the beam is decreased.

5.3 Effect of radius of curvature of beam on fundamental natural frequency (L/R)

Decreasing radius of curvature (R) increased the amount of fundamental natural frequency; i.e., the straight beam had the lowest natural frequencies and, increasing the curvature made the system stiffer. These variations for h_c/h=0.8 and L/h=10 are plotted in Fig. 4.

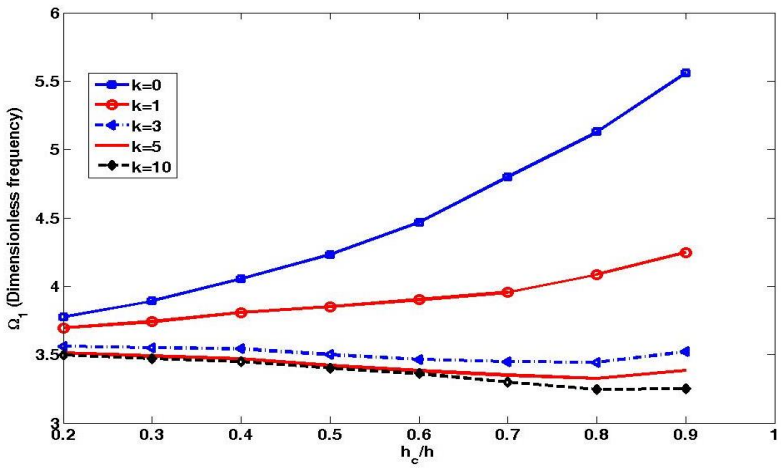

Fig. 2 Variations of fundamental natural frequencies of a sandwich curved beam with respect to core to beam thickness ratio

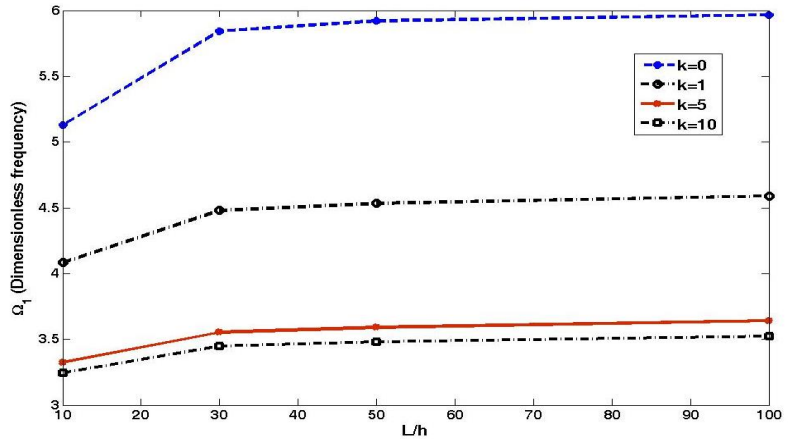

Fig. 3 Variations of fundamental natural frequencies of a sandwich curved beam with respect to length to thickness ratio

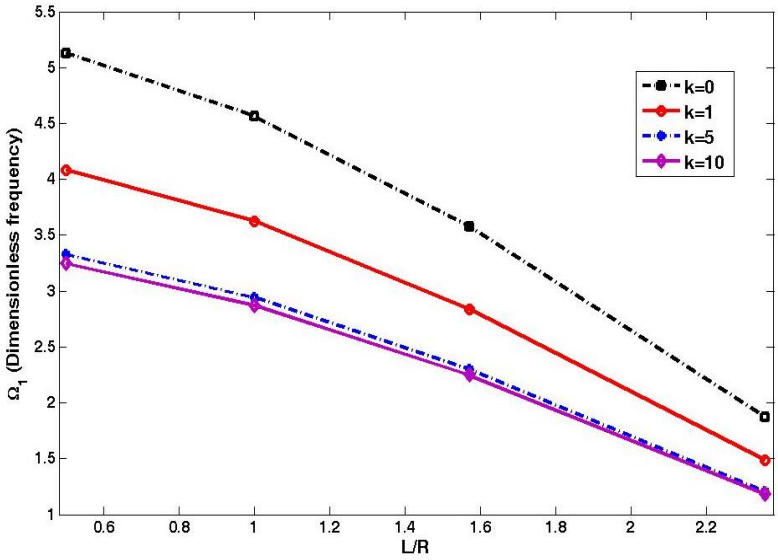

Fig. 4 Variations of fundamental natural frequencies of a sandwich curved beam with FG core with respect to length to radius ratio

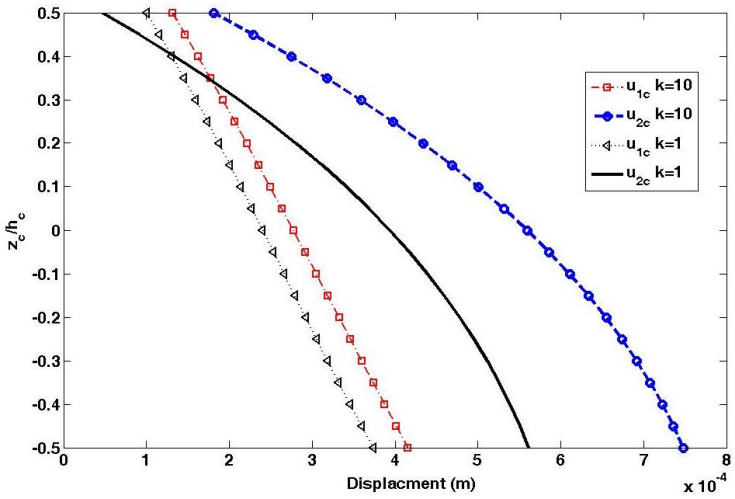

Fig. 5 Axial displacement of the core for two amounts of k and for two first modes

5.4 Effect of variations of k on modal axial displacement of core, u_c for the two first natural frequencies

Fig. 5 shows modal axial displacement of the core by variations of k (FG-core parameter). u_{1c} is axial displacement related to the first natural frequency and u_{2c} for the second one. These displacements were measured from the middle of the curved beam and were plotted based on the ratios of z_c/h_c. u_c is calculated based on the displacement field in Eq. (4). As can be seen, modal

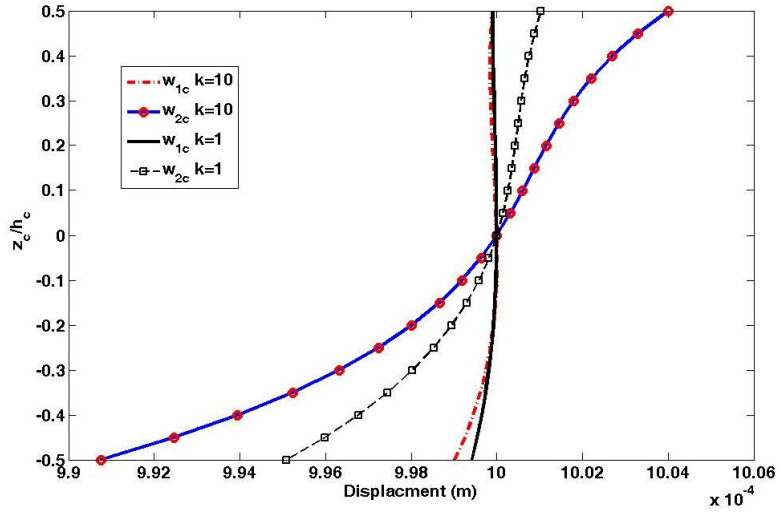

Fig. 6 Radial displacement of the core for two amounts of *k*, and for two first modes

axial displacement of the core on the top region was greater than the bottom region for all the mode shapes; so, the displacement on the region of the top face-sheet was not equal to the region of the bottom face-sheet, which was the result of non-homogeneous (FG) material distribution through thickness of the core.

5.5 Effect of variations of k on modal radial displacement of core, w_c, for the two first natural frequencies

Radial displacement of the core based on the displacement field in Eq. (4) is plotted in Fig. 6 for various *k* factors and two first modes. It shows that the modal radial displacement for the second mode had more variation by increasing *k* factor compared to the first mode.

6. Conclusions

Vibration of cross-ply laminated composite and sandwich curved beams with FG cores on the basis of 2D refined higher order beam theory (RHOBT) was studied for simply supported boundary conditions. The characteristic eigenvalue governing equation was obtained based on Hamilton's principle using Fourier series solution method. Since the cross-sectional warping was accurately modeled by this theory, it did not require any shear correction factor. Also, the present analysis incorporated trapezoidal shape factor (the 1+z/R terms) of a curved beam element that arose due to the fact that stresses over the beam thickness were to be integrated on cross-section of a curved beam element to obtain accurate stress-resultants. The solutions were also applicable to straight beams by taking radius of curvature as infinity. Comparisons of the results for thin and thick curved beams with the published results in the literature were carried out and good agreement was observed. Variations of some parameters which could affect fundamental natural frequency of the system were also investigated:

- Thickness of core: Increasing thickness of the core compared to thickness of the beam could increase or decrease fundamental natural frequency, depending on the amount of *k* (FG-core parameter) factor.

- Length of beam: Increasing this parameter affected fundamental natural frequency by increasing it, but in a decreasing ratio.

- Radius of curvature: Higher radius of curvature led a lower amount of fundamental natural frequency. Also, axial and radial displacements of the core for two first modes were plotted to show effect of non-homogeneous material distribution through thickness of the FGM-core which caused displacements on the region of the top face-sheet not to be equal to the region of the bottom face-sheet. The present method does not require any convergence study, in contrast to some other higher-order theories for free vibration analyses reported in the literature. So, the present method could be effectively used for design purposes, where short run-time is important like structural optimization procedures.

8. References

Ahmed, K.M. (1971), "Free vibration of curved sandwich beams by the method of finite elements", *J. Sound. Vib.*, **18**, 61-74.

Apetre, N.A., Sankar, B.V. and Ambur, D.R. (2006), "Low-velocity impact of sandwich beams with functionally graded core", *Int. J. Solid. Struct.*, **43**(9), 2479-2496.

Aydogdu, M. and Taskin, V. (2007), "Free vibration analysis of functionally graded beams with simply supported edges", *Mater. Des.*, **28**(5), 1651-1656.

Auciello, N.M. and Rosa, M.A. (1994), "Free vibrations of circular arches: a review", *J. Sound. Vib.*, **176**, 433-458.

Bao, G. and Wang, L. (1995), "Multiple cracking in functionally graded ceramic/metal coatings", *Int. J. Solid. Struct.*, **32**, 2853-2871.

Balasubramanian, T.S. and Prathap, G. (1989), "A field consistent higher-order curved beam element for static and dynamic analysis of stepped arches", *J. Comput. Struct*., **33**, 281-288.

Birman, V. (1995), "Stability of functionally graded hybrid composite plates", *Compos. Eng.*, **5**, 913-921.

Chi, S.H. and Chung, Y.L. (2003), "Cracking in coating substrate composites of multi layered and sigmoid FGM coatings", *Eng. Fract. Mech.*, **70**, 1227-1243.

Eisenberger, M. and Efraim, E. (2001), "In-plane vibrations of shear deformable curved beams", *Int. J. Numer. Meth. Eng.*, **52**, 1221-1234.

Garg, A.K., Khare, R.K. and Kant, T. (2006), "Higher-order closed-form solutions for free vibration of laminated composite and sandwich shells", *J. Sandwich Struct. Mater.*, **8**(3), 205-235.

Golmakani, M.E. and Kadkhodayan, M.E. (2011), "Nonlinear bending analysis of annular FGM plates using higher-order shear deformation plate theories", *Compos. Struct.*, **93**, 973-982.

Kang, B., Riedel, C.H. and Tan, C.A. (2003), "Free vibration analysis of planar curved beams by wave propagation", *J. Sound. Vib.*, **260,** 19-44.

Henrych, J. (1981), *The Dynamics of Arches*, Elsevier Frames, New York.

Khdeir, A.A. and Reddy, J.N. (1997), "Free and forced vibration of cross-ply laminated composite shallow arches", *Int. J. Solid. Struct*., **34**, 1217-1234.

Kiani, Y., Akbarzadeh, A.H., Chen, Z.T. and Eslami, M.R. (2012), "Static and dynamic analysis of an FGM doubly curved panel resting on the Pasternak type elastic foundation", *Compos. Struct.*, **94**, 2474-2484.

Koizumi, M. (1993), "The concept of FGM ceramic transactions: functionally gradient materials", **34**, 3-10.

Khalili, S.M.R., Tafazoli, S. and Malekzadeh Fard, K. (2011), "Free vibrations of laminated composite shells with distributed uniformly attached mass using higher order shell theory including stiffness effect", *J. Sound. Vib.*, **330**(26), 6355-6371.

Krishnan, A, Dharmaraj, S. and Suresh, Y.J. (1995), "Free vibration studies of arches", *J. Sound. Vib.*, **186**, 856-863.

Krishnan, A. and Suresh, Y.J. (1998), "A simple cubic linear element for static and free vibration analyses of curved beams", *J. Comput. Struct.*, **68**, 473-489.

Li, X.F. (2008), "A unified approach for analyzing static and dynamic behaviors of functionally graded Timoshenko and Euler-Bernoulli beams" , *J. Sound. Vib.*, **318**, 1210-29.

Lu, Q. and Lu, C.F. (2008), "Exact two-dimensional solutions for in-plane natural frequencies of laminated circular arches", *J. Sound. Vib.*, **318**, 982-990.

Malekzadeh, P. (2009), "Two-dimensional in-plane free vibrations of functionally graded circular arches with temperature-dependent properties", *Compos. Struct.*, **91**, 38-47.

Malekzadeh, P., Golbahar Haghighi, M.R. and Atashi, M.M. (2010), "Out of plane free vibration of functionally graded circular curved beam in thermal environment", *Compos. Struct.*, **92**, 541-552.

Marur, S.R. and Kant, T. (2008), "Free vibration of higher-order sandwich and composite arches, Part I: formulation" , *J. Sound. Vib*., **310**(1-2), 91-109.

Mori, T. and Tanaka, K. (1973), "Average stress in the matrix and average elastic energy of materials with misfitting inclusions", *Acta Metall*., **21**, 571-574.

Qatu, M.S. (1993), "Theories and analysis of thin and moderately thick laminated composite curved beams", *Int. J. Solid. Struct*., **30**(3), 2743-2756.

Sakiyama, T., Matsuda, H. and Morita, C. (1997), "Free vibration analysis of sandwich arches with elastic or visco elastic core and various kinds of axis shape and boundary conditions", *J. Sound. Vib*., **203**, 505-522.

Sankar, B.V. (2001), "An elasticity solution for functionally graded beams", *Compos. Sci. Technol.*, **61**(5), 689-696.

Shen, H.S. (2009), *Functionally Graded Materials-Nonlinear Analysis of Plates and Shells*, CRC Press.

Tseng, Y.P., Huang, C.S. and Kao, M.S. (2000), "In-plane vibration of laminated curved beams with variable curvature by dynamic stiffness analysis", *J. Compos. Struct*., **50**, 103-114.

Appendix A. Definition of D matrices

The terms H_j, $\hat{H}_j$ and $\overline{H}_j$ (j=1, 2, …, 7), used in the following matrices ($\mathbf{D_f}$ and $\mathbf{D_s}$), are defined in Appendix B.

$$\mathbf{D}_{\mathbf{f}\ 7\times7}=\sum_{k=1}^{NL}\begin{bmatrix} Q_{11}\overline{H}_1 & Q_{11}\overline{H}_3 & Q_{12}H_1 & Q_{12}H_3 & Q_{11}\overline{H}_2 & Q_{11}\overline{H}_4 & Q_{12}H_2 \\ Q_{11}\overline{H}_3 & Q_{11}\overline{H}_5 & Q_{12}H_3 & Q_{12}H_5 & Q_{11}\overline{H}_4 & Q_{11}\overline{H}_6 & Q_{12}H_4 \\ Q_{21}H_1 & Q_{21}H_3 & Q_{22}\hat{H}_1 & Q_{22}\hat{H}_3 & Q_{21}H_2 & Q_{21}H_4 & Q_{22}\hat{H}_2 \\ Q_{21}H_3 & Q_{21}H_5 & Q_{22}\hat{H}_3 & Q_{22}\hat{H}_5 & Q_{21}H_4 & Q_{21}H_6 & Q_{22}\hat{H}_4 \\ Q_{11}\overline{H}_2 & Q_{11}\overline{H}_4 & Q_{12}H_2 & Q_{12}H_4 & Q_{11}\overline{H}_3 & Q_{11}\overline{H}_5 & Q_{12}H_3 \\ Q_{11}\overline{H}_4 & Q_{11}\overline{H}_6 & Q_{12}H_4 & Q_{12}H_6 & Q_{11}\overline{H}_5 & Q_{11}\overline{H}_7 & Q_{12}H_5 \\ Q_{21}H_2 & Q_{21}H_4 & Q_{22}\hat{H}_2 & Q_{22}\hat{H}_4 & Q_{21}H_3 & Q_{21}H_5 & Q_{22}\hat{H}_3 \end{bmatrix}^k$$

$$\mathbf{D}_{\mathbf{s}\ 7\times7}=\sum_{k=1}^{NL}Q_{33}\begin{bmatrix} \overline{H}_1 & H_1 & \overline{H}_3 & H_3 & \overline{H}_2 & H_2 & \overline{H}_4 \\ & \hat{H}_1 & H_3 & \hat{H}_3 & H_2 & \hat{H}_2 & H_4 \\ & & \overline{H}_5 & H_5 & \overline{H}_4 & H_4 & \overline{H}_6 \\ & & & \hat{H}_5 & H_4 & \hat{H}_4 & H_6 \\ & & & & \overline{H}_3 & H_3 & \overline{H}_5 \\ & & & & & \hat{H}_3 & H_5 \\ & & \textit{sym.} & & & & \overline{H}_7 \end{bmatrix}^k$$

Appendix B. Definition of H components

In matrices $\mathbf{D_f}$, and $\mathbf{D_s}$ the terms H_j, $\hat{H}_j$ and $\overline{H}_j$ are defined as follows:

B.1 Definition of H_j

$$H_j=\int_{h_k}^{h_{k+1}} z^{j-1}dz=\frac{(h_{k+1}^j-h_k^j)}{j} \qquad , \qquad j=1,2,...,6 \tag{B.1}$$

B.2 Definition of $\hat{H}_j$

$$\hat{H}_j=\int_{h_k}^{h_{k+1}} z^{j-1}\left(1+z/R\right)dz=H_j+\frac{1}{R}H_{j+1} \qquad , \qquad j=1,2,...,6 \tag{B.2}$$

where H_j are defined in Eq. (B.1).

B.3 Definition of $\overline{H}_j$

$$\overline{H}_j = \int_{h_k}^{h_{k+1}} \frac{z^{j-1}}{\left(1+z/R\right)} dz \quad , \quad j = 1,2,...,7 \tag{B.3}$$

Here, exact integration method for calculating the integral in Eq. (B.3) is applied for calculating the stress-resultants used in the refined higher-order beam theory. In this method, the integral in Eq. (B.3) is calculated accurately. After taking exact integration, the following results are obtained:

$$\overline{H}_1 = \int_{h_k}^{h_{k+1}} \frac{1}{\left(1+z/R\right)} dz = R\left[\ln\left(\frac{R+h_{k+1}}{R+h_k}\right)\right]$$

$$\overline{H}_2 = \int_{h_k}^{h_{k+1}} \frac{z}{\left(1+z/R\right)} dz = R\left[\left(h_{k+1}-h_k\right) - R\ln\left(\frac{R+h_{k+1}}{R+h_k}\right)\right]$$

$$\overline{H}_3 = \int_{h_k}^{h_{k+1}} \frac{z^2}{\left(1+z/R\right)} dz = R\left[\frac{1}{2}\left(h_{k+1}^2-h_k^2\right) - R\left(h_{k+1}-h_k\right) + R^2\ln\left(\frac{R+h_{k+1}}{R+h_k}\right)\right]$$

$$\overline{H}_4 = \int_{h_k}^{h_{k+1}} \frac{z^3}{\left(1+z/R\right)} dz = R\left[\frac{1}{3}\left(h_{k+1}^3-h_k^3\right) - \frac{1}{2}R\left(h_{k+1}^2-h_k^2\right) + R^2\left(h_{k+1}-h_k\right) - R^3\ln\left(\frac{R+h_{k+1}}{R+h_k}\right)\right]$$

$$\overline{H}_5 = \int_{h_k}^{h_{k+1}} \frac{z^4}{\left(1+z/R\right)} dz = R\left[\begin{array}{l}\frac{1}{4}\left(h_{k+1}^4-h_k^4\right) - \frac{1}{3}R\left(h_{k+1}^3-h_k^3\right) + \frac{1}{2}R^2\left(h_{k+1}^2-h_k^2\right) - R^3\left(h_{k+1}-h_k\right) \\ + R^4\ln\left(\frac{R+h_{k+1}}{R+h_k}\right)\end{array}\right]$$

$$\overline{H}_6 = \int_{h_k}^{h_{k+1}} \frac{z^5}{\left(1+z/R\right)} dz = R\left[\begin{array}{l}\frac{1}{5}\left(h_{k+1}^5-h_k^5\right) - \frac{1}{4}R\left(h_{k+1}^4-h_k^4\right) + \frac{1}{3}R^2\left(h_{k+1}^3-h_k^3\right) - \frac{1}{2}R^3\left(h_{k+1}^2-h_k^2\right) \\ + R^4\left(h_{k+1}-h_k\right) - R^5\ln\left(\frac{R+h_{k+1}}{R+h_k}\right)\end{array}\right]$$

$$\overline{H}_7 = \int_{h_k}^{h_{k+1}} \frac{z^6}{\left(1+z/R\right)} dz = R\left[\begin{array}{l}\frac{1}{6}\left(h_{k+1}^6-h_k^6\right) - \frac{1}{5}R\left(h_{k+1}^5-h_k^5\right) + \frac{1}{4}R^2\left(h_{k+1}^4-h_k^4\right) - \frac{1}{3}R^3\left(h_{k+1}^3-h_k^3\right) \\ + \frac{1}{2}R^4\left(h_{k+1}^2-h_k^2\right) - R^5\left(h_{k+1}-h_k\right) + R^6\ln\left(\frac{R+h_{k+1}}{R+h_k}\right)\end{array}\right] \tag{B.4}$$

Appendix C. Elements of stiffness and mass matrices

C.1 Some elements of stiffness matrix $\boldsymbol{K}_{8x8}$

$$K_{45}=(-\frac{1}{R^2}D_{f52}-\frac{1}{R}D_{f32}-\frac{1}{R^2}D_{s53}+\frac{2}{R}D_{s56})(-\lambda),\quad K_{46}=C_1[(\frac{1}{R^2}D_{s53})(-\lambda^2)$$
$$+(-\frac{2}{R}D_{f57}-\frac{1}{R^2}D_{f52}-\frac{1}{R}D_{f32}-2D_{f37})],\quad K_{47}=(-\frac{1}{R^2}D_{f56}-\frac{1}{R}D_{f36}+\frac{3}{R}D_{s54} \tag{C.1}$$
$$-\frac{1}{R^2}D_{s57})(-\lambda),\quad K_{48}=C_2[(\frac{1}{R^2}D_{s57})(-\lambda^2)+(-\frac{3}{R}D_{f54}-\frac{1}{R^2}D_{f56}-\frac{1}{R}D_{f36}-3D_{f34})]$$

$$K_{11}=(\frac{1}{R^2}D_{f11}+\frac{\gamma_0}{R^3}D_{f15}+\frac{\gamma_0}{R^3}D_{f51}+\frac{\gamma_0}{R^4}D_{f55})(-\lambda^2)+(-\frac{1}{R^2}D_{s11}+\frac{\gamma_0}{R^2}D_{s12}-\frac{\gamma_0}{R^3}D_{s15}$$
$$-\frac{\gamma_0}{R^3}D_{s51}+\frac{\gamma_0}{R^3}D_{s52}-\frac{\gamma_0}{R^4}D_{s55}+\frac{\gamma_0}{R^2}D_{s21}-\frac{\gamma_0}{R^2}D_{s22}+\frac{\gamma_0}{R^3}D_{s25})$$
$$K_{14}=C_1[(\frac{1}{R}D_{f13}+\frac{1}{R^2}D_{f15}+\frac{1}{R^2}D_{s15}+\frac{\gamma_0}{R^2}D_{f53}+\frac{\gamma_0}{R^3}D_{f55}+\frac{\gamma_0}{R^3}D_{s55}-\frac{\gamma_0}{R^2}D_{s25})(\lambda)] \tag{C.2}$$
$$K_{15}=(\frac{1}{R^2}D_{f12}+\frac{\gamma_0}{R^3}D_{f52})(-\lambda^2)+(-\frac{1}{R^2}D_{s13}+\frac{2}{R}D_{s16}-\frac{\gamma_0}{R^3}D_{s53}+2\frac{\gamma_0}{R^2}D_{s56}+\frac{\gamma_0}{R^2}D_{s23}$$
$$-2\frac{\gamma_0}{R}D_{s26}),\quad K_{16}=C_1[(\frac{1}{R^2}D_{f12}+\frac{2}{R}D_{f17}+\frac{1}{R^2}D_{s13}+\frac{\gamma_0}{R^3}D_{f52}+2\frac{\gamma_0}{R^2}D_{f57}+\frac{\gamma_0}{R^3}D_{s53}$$

C.2 Some elements of Mass matrix $\boldsymbol{M}_{8x8}$

$$M_{11}=(\bar{I}_0+\frac{2\gamma_0}{R}\bar{I}_1+\frac{\gamma_0}{R^2}\bar{I}_2),\quad M_{13}=(\bar{I}_1+\frac{\gamma_0}{R}\bar{I}_2),\quad M_{15}=(\bar{I}_2+\frac{\gamma_0}{R}\bar{I}_3),\quad M_{17}=(\bar{I}_3+\frac{\gamma_0}{R}\bar{I}_4);$$
$$M_{22}=\bar{I}_0,\quad M_{24}=\bar{I}_1,\quad M_{26}=\bar{I}_2,\quad M_{28}=\bar{I}_3;\quad M_{31}=(\bar{I}_1+\frac{\gamma_0}{R}\bar{I}_2),\quad M_{33}=\bar{I}_2,\quad M_{35}=\bar{I}_3,$$
$$M_{37}=\bar{I}_4;\quad M_{42}=\bar{I}_1,\quad M_{44}=\bar{I}_2,\quad M_{46}=\bar{I}_3,\quad M_{48}=\bar{I}_4;\quad M_{51}=(\bar{I}_2+\frac{\gamma_0}{R}\bar{I}_3),\quad M_{53}=\bar{I}_3, \tag{C.3}$$
$$M_{55}=\bar{I}_4,\quad M_{57}=\bar{I}_5;\quad M_{62}=\bar{I}_2,\quad M_{64}=\bar{I}_3,\quad M_{66}=\bar{I}_4,\quad M_{68}=\bar{I}_5;\quad M_{71}=(\bar{I}_3+\frac{\gamma_0}{R}\bar{I}_4)$$
$$M_{73}=\bar{I}_4,\quad M_{75}=\bar{I}_5,\quad M_{77}=\bar{I}_6;\quad M_{82}=\bar{I}_3;\quad M_{84}=\bar{I}_4;\quad M_{86}=\bar{I}_5;\quad M_{88}=\bar{I}_6;$$